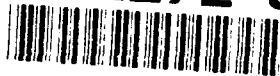


AD-A272 921



AAMRL-TR-89-004



THIN FILM PHOSPHOR DEVELOPMENT (U)

J. SHMULOVICH

AT&T BELL LABORATORIES
MURRAY HILL, NJ 07974

JANUARY 1989

PERIOD OF PERFORMANCE: JANUARY 1987 - DECEMBER 1988

93-28484



Approved for public release; distribution is unlimited.

HARRY G. ARMSTRONG AEROSPACE MEDICAL RESEARCH LABORATORY
HUMAN SYSTEMS DIVISION
AIR FORCE SYSTEMS COMMAND
WRIGHT-PATTERSON AIR FORCE BASE, OHIO 45433-6573

**Best
Available
Copy**

NOTICES

When US Government drawings, specifications, or other data are used for any purpose other than a definitely related Government procurement operation, the Government thereby incurs no responsibility nor any obligation whatsoever, and the fact that the Government may have formulated, furnished, or in any way supplied the said drawings, specifications, or other data, is not to be regarded by implication or otherwise, as in any manner licensing the holder or any other person or corporation, or conveying any rights or permission to manufacture, use, or sell any patented invention that may in any way be related thereto.

Please do not request copies of this report from Armstrong Aerospace Medical Research Laboratory. Additional copies may be purchased from:

National Technical Information Service
5285 Port Royal Road
Springfield, Virginia 22161

Federal Government agencies and their contractors registered with Defense Technical Information Center should direct requests for copies of this report to:

Defense Technical Information Center
Cameron Station
Alexandria, Virginia 22314

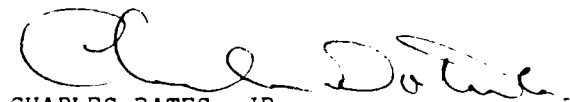
TECHNICAL REVIEW AND APPROVAL

AAMRL-TR-89-004

This report has been reviewed by the Office of Public Affairs (PA) and is releasable to the National Technical Information Service (NTIS). At NTIS, it will be available to the general public, including foreign nations.

This technical report has been reviewed and is approved for publication.

FOR THE COMMANDER



CHARLES BATES, JR.
Director, Human Engineering Division
Armstrong Aerospace Medical Research Laboratory

UNCLASSIFIED

SECURITY CLASSIFICATION OF THIS PAGE

REPORT DOCUMENTATION PAGE

1. REPORT SECURITY CLASSIFICATION UNCLASSIFIED		1b. RESTRICTIVE MARKINGS	
2a. SECURITY CLASSIFICATION AUTHORITY		3. DISTRIBUTION/AVAILABILITY OF REPORT Approved for public release; distribution is unlimited.	
2b. DECLASSIFICATION/DOWNGRADING SCHEDULE			
4. PERFORMING ORGANIZATION REPORT NUMBER(S) -		5. MONITORING ORGANIZATION REPORT NUMBER(S) AAMRL-TP-89-004	
5a. NAME OF PERFORMING ORGANIZATION AT&T Bell Laboratories	6a. OFFICE SYMBOL (If applicable)	7a. NAME OF MONITORING ORGANIZATION AAMRL/HEA	
5b. ADDRESS (City, State and ZIP Code) Murray Hill, NJ 07974		7b. ADDRESS (City, State and ZIP Code) Wright-Patterson AFB OH 45433-6573	
8a. NAME OF FUNDING/SPONSORING ORGANIZATION	8b. OFFICE SYMBOL (If applicable)	9. PROCUREMENT INSTRUMENT IDENTIFICATION NUMBER F33615-84-C-0503	
8c. ADDRESS (City, State and ZIP Code)		10. SOURCE OF FUNDING NOS	
		PROGRAM ELEMENT NO	PROJECT NO
		62202F	7814
		TASK NO	WORK UNIT NO
		11	48
11. TITLE (Include Security Classification) THIN FILM PHOSPHOR DEVELOPMENT (U)			
12. PERSONAL AUTHOR(S) SHMULOVICH, J.			
13a. TYPE OF REPORT Summary	13b. TIME COVERED FROM Jan 87 TO Dec 88	14. DATE OF REPORT (Yr., Mo., Day) 89 Jan	15. PAGE COUNT 31
16. SUPPLEMENTARY NOTATION			
7. COSATI CODES		18. SUBJECT TERMS (Continue on reverse if necessary and identify by block number)	
FIELD	GROUP	SUB. GR.	
09	05		
		cathodoluminescence, sputtered phosphors, helmet-mounted displays, head-up displays, light output coupling, cathode-ray-tubes	
9. ABSTRACT (Continue on reverse if necessary and identify by block number)			
Thin poly-crystalline phosphor films are capable of high brightness and resolution in severe application conditions. The program described here concentrated on sputter-deposition of $Tb^{3+}:Y_3Al_3Ga_2O_{12}$ phosphor. The problem of optical contact of the film with the substrate was addressed in optical isolation schemes.			
0. DISTRIBUTION/AVAILABILITY OF ABSTRACT UNCLASSIFIED/UNLIMITED <input checked="" type="checkbox"/> SAME AS RPT. <input type="checkbox"/> DTIC USERS <input type="checkbox"/>		21. ABSTRACT SECURITY CLASSIFICATION UNCLASSIFIED	
2a. NAME OF RESPONSIBLE INDIVIDUAL Dean F. Kocian	22b. TELEPHONE NUMBER (Include Area Code) (513)255-8904	22c. OFFICE SYMBOL AAMRL/HEA	

SUMMARY

This report is the final in a series of reports that investigated the structure, activation mechanisms, and performance of single-crystal phosphors (SCPs) and thin film poly-crystalline (sputtered) phosphors with respect to their application in miniature high resolution/luminance cathode-ray-tubes (CRTs). It covers work relating to the development of sputtered $\text{Tb}^{3+}:\text{Y}_3\text{Al}_5\text{O}_{12}$ (YAG) and $\text{Tb}^{3+}:\text{Y}_3\text{Al}_3\text{Ga}_2\text{O}_{12}$ (YAGG) thin film poly-crystalline phosphors. The report separates the phosphor development process and CRT performance assessment into two stages: stage (1) dealing with learning how to deposit efficient and stable phosphor layers using thin film techniques, and stage (2) dealing with maximizing the external light transmission efficiency by solving the optical contact problem arising from the index of refraction mismatch between the phosphor, substrate, and transmission medium. The author clearly shows that successful deposition techniques were demonstrated for both the YAG and YAGG phosphors and that internal light conversion efficiency was equal to or better than the best particulate phosphors. In addition, the life characteristics or Coulombic degradation parameter was greatly improved over that found in conventional phosphors. However, the two approaches used for solving the optical contact problem, optical isolation structures and anti-halo filters, were not successful because of the high phosphor annealing temperatures (1300°C) needed to obtain the best luminous efficiency. On the plus side, the author does show that the external luminance performance observed for the thin-film phosphors, using only the basic sapphire faceplate, does compare almost exactly with particulate phosphors up to respectable power levels before saturation effects become noticeable in the thin-film phosphor, and in any event, line width is always smaller for the thin-film phosphor. Finally, the report proposes methods for reducing processing temperatures that might permit the solution of the optical contact problem with known materials. The successes achieved during this program suggest that thin film phosphors are worthy of serious consideration for at least some miniature CRT applications.

Accession For	
NTIS CRA&I	<input checked="" type="checkbox"/>
DTIC TAB	<input checked="" type="checkbox"/>
Unannounced	<input type="checkbox"/>
Justification	
By	
Distribution/	
Availability Codes	
Dist	Available or Special
A-1	

PREFACE

The technical work recorded in this report was performed and summarized by J. Shmulovich, Member of Technical Staff at AT&T Bell Laboratories.

This contract, F33615-84-C-0503, is conducted for the Air Force under the technical direction of Mr. Dean Kocian, project engineer, AAMRL. The technical program at AT&T Bell Laboratories is under the direction of S. L. Blank and W. E. Hess.

TABLE OF CONTENTS

I.	INTRODUCTION	1
II.	SPUTTER-DEPOSITION OF Tb^{3+} :YAGG FILMS	2
	1 Experimental	2
	2 Experimental Results	2
	3 CRT Performance	9
	4 Discussion	9
III.	OPTICAL ISOLATION STRUCTURE	13
	1 Introduction	13
	2 Experimental Results and Discussion	15
IV.	ANTI-HALO FILTER FOR THIN-FILM PHOSPHORS	18
V.	CONCLUSION	20
	REFERENCES	22
	APPENDIX	23

LIST OF ILLUSTRATIONS

Figure	Description	Page
1	X-ray spectra of sputtered Tb ³⁺ :YAGG films	3
2	Raster brightness of Tb ³⁺ :YAGG and Tb ³⁺ :YAG films	4
3	Decay of Tb ³⁺ (⁵ D ₄) emission intensity versus time	6
4	An SEM microphotograph of Tb ³⁺ :YAGG film	7
5	Peak line Brightness and FWHM of commercial P53 and Tb ³⁺ :YAGG film ...	10
6	Schematic presentation of an optical isolation structure	14
7	Optical microphotograph of Tb ³⁺ :YAGG film on SiO ₂ layer	16
8	An SEM microphotograph of Tb ³⁺ :YAGG film on SiO ₂ layer	16
9	X-ray spectra of Tb ³⁺ :YAGG on SiO ₂ layer	17
10	X-ray spectra of Tb ³⁺ :YAGG on SiO ₂ layer	19

LIST OF TABLES

Number	Description	Page
1	Relative brightness of $\text{Tb}^{3+}:\text{YAG}$ and $\text{Tb}^{3+}:\text{YAGG}$ phosphors	5
2	RBS analysis results of $\text{Tb}^{3+}:\text{YAGG}$ films	8

I. INTRODUCTION

Cathodoluminescent materials deposited in the form of translucent thin films have a number of important advantages over particulate ("powder") phosphors of the same composition in high brightness, high resolution cathode-ray tube (CRT) applications.^[1] They provide a more efficient heat transfer from the phosphor to the faceplate, longer life, and higher resolution. In a previous report^[1] we described our results on successful deposition of $\text{Tb}^{3+}:\text{Y}_3\text{Al}_5\text{O}_{12}$ ($\text{Tb}^{3+}:\text{YAG}$) cathodoluminescent thin films on sapphire substrates by an RF sputtering technique. In these films an improvement of a factor of two in the external efficiency and an internal conversion efficiency matching that of an analogous single crystal phosphor were achieved.

Equally important, the new thin film phosphor proved to be superior to its powder analog in electron beam induced deterioration. Long term loss of efficiency of the phosphor upon e-beam bombardment is known as coulombic degradation. It is measured in amounts of charge deposited per unit area that causes a 50% decrease in the efficiency of the phosphor.^[2] The luminous efficiency of the film dropped only 3% after 700 Coulombs(C)/ cm^2 electron irradiation dose. This compares to a drop of 50% after 200 Coulombs(C)/ cm^2 irradiation observed for commercial $\text{Tb}^{3+}:\text{YAG}$ powder phosphors.^[3]

Powder $\text{Tb}^{3+}:\text{YAG}$ is an efficient green narrow-band emitting phosphor with high quenching temperature and the longest coulombic lifetime^[3,4] of any particulate phosphor. For these reasons it is widely used in commercial and military displays. However, new higher brightness green phosphors such as $\text{Tb}^{3+}:\text{Y}_3\text{Al}_3\text{Ga}_2\text{O}_{12}$ ($\text{Tb}^{3+}:\text{YAGG}$),^[5] $\text{Tb}^{3+}:\text{Y}_2\text{SiO}_5$,^[6] $\text{Tb}^{3+}:\text{LaOCl}$ ^[7] were developed recently that are sufficiently stable under e-beam bombardment. Of these, $\text{Tb}^{3+}:\text{YAGG}$ (TEPAC designation P53^[8]) has become the phosphor of choice in many high brightness applications. Our previous work on $\text{Tb}^{3+}:\text{YAG}$, aside from producing an efficient and long-lived cathodoluminescent film, which has significant value in itself, laid a foundation for the sputter-deposition of $\text{Tb}^{3+}:\text{YAGG}$. The latter phosphor is chemically more complex and, therefore, potentially more difficult to deposit than $\text{Tb}^{3+}:\text{YAG}$.

The results on sputter-deposition and evaluation of $\text{Tb}^{3+}:\text{Y}_3\text{Al}_3\text{Ga}_2\text{O}_{12}$ thin films are reported in Section 2. A number of CRT's with sputtered $\text{Tb}^{3+}:\text{YAGG}$ faceplates were built and their performance is compared to that of conventional state-of-the-art tubes.

The drawback of thin film phosphors is that their optical contact with the faceplate^[9] decreases the external efficiency of the phosphor. The second part of this report will concentrate on two approaches directed toward improving the light extraction efficiency of the films. They both make use of light scattering by the film to increase the light output.

In Section 3 we will introduce the concept of optical isolation layers, and will present the results of our effort to fabricate them. In Section 4 we will discuss a different approach to the problem of optical contact that utilizes multilayer interference filters to redirect the emitted light toward the observer. Our effort to build such a faceplate with the help of an outside vendor is also summarized.

II. SPUTTER-DEPOSITION OF Tb^{3+} :YAGG FILMS

1. Experimental

The films were sputtered in a Materials Research Corporation 8620 sputtering system that was modified by installation of an Anelva 3-inch diameter planar magnetron instead of the original target assembly. The system was evacuated to better than 1×10^{-6} torr with a Varian VHS6 diffusion pump utilizing a liquid nitrogen trap filled around-the-clock.

A three inch melted and quenched ($\text{Y}_{2.85}\text{Tb}_{0.15}$) $\text{Al}_3\text{Ga}_2\text{O}_{12}$ disk was used as a target in the majority of experiments. RF power densities at the target were 4.5-14 W/cm^2 . The substrates were 1-inch diameter 0.020 inch-thick sapphire disks. They were placed on an electrically grounded stainless steel plate that could be heated during the deposition. A thermocouple was clamped at the edge of the plate to monitor the plate's temperature. The typical deposition rate was about 70-200 $\text{\AA}/\text{min}$ and did not vary significantly with oxygen content or the total gas pressure.

The sputtering was done in an atmosphere of argon and oxygen, where the oxygen concentration in the mixture was varied from zero to 20%. Total gas mixture pressures from 10 mtorr to 50 mtorr were used in the experiments. Air Products research grade argon (99.9995%) and oxygen (99.996%) were used without additional purification and the gases were not premixed before entering the sputtering chamber. The deposited films were fired in air at temperatures ranging from 900°C to 1300°C. The set temperature was reached in about two hours and the samples were soaked at that temperature for two hours. The furnace was then shut-off and samples cooled to the room temperature in about seven hours. Structural, spectral and luminescent properties of the films were studied as a function of deposition parameters and heat treatment, as described in Ref. 1. A number of CRT's with 1-inch diameter sputtered faceplates were fabricated and evaluated.

2. Experimental Results

As deposited Tb^{3+} :YAGG films were amorphous and crystallized upon heat treatment. The development of the the x-ray diffraction pattern as a function of the firing temperature can be followed in Fig. 1. Two different garnet phases are observed in the fired films. The "low temperature" phase observed in the film treated at 900°C has a larger lattice constant than the "high temperature" phase developed in the film annealed at 1300°C, as follows from the shift of the x-ray lines. The high temperature phase grows at the expense of the low temperature phase with the increase in firing temperature, and at intermediate temperatures both phases are present. The brightness of a typical sputtered Tb^{3+} :YAGG film is given in Fig. 2 as a function of the firing temperature. In the same figure, similar results for a sputtered Tb^{3+} :YAG film are shown. Note that the brightness of the Tb^{3+} :YAGG film increases 15.5 times as the firing temperature rises from 900° to 1300°C, whereas that of the Tb^{3+} :YAG increases only 5 times. This result may indicate that the high temperature phase of Tb^{3+} :YAGG has a higher cathodoluminescence efficiency than the low temperature one. This

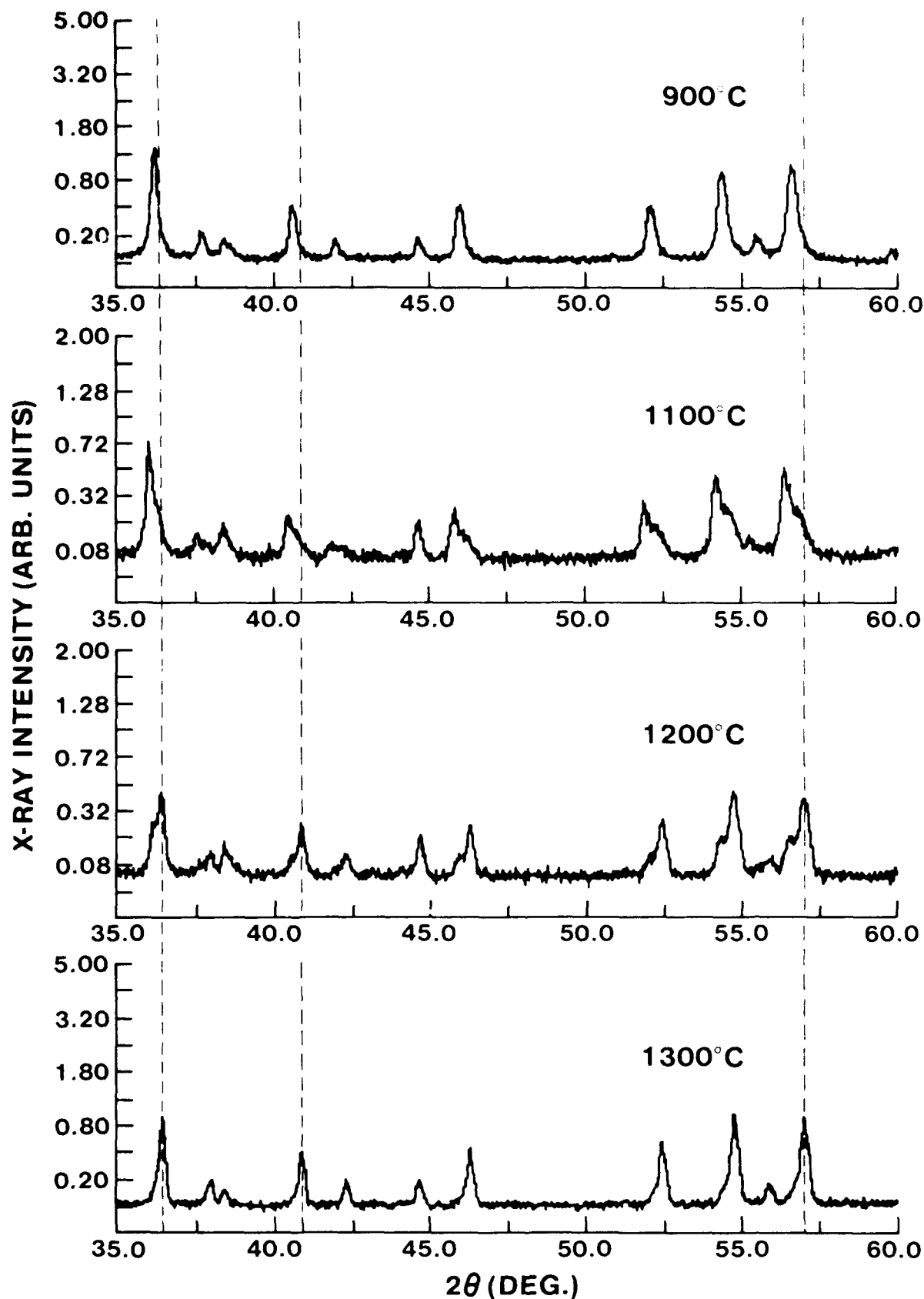


Figure 1 X-ray powder diffraction spectra of sputtered $\text{Tb}^{3+}:\text{YAGG}$ films fired for 2 hours in air at the temperature indicated at the figure. The thin vertical lines mark the position of the selected diffraction peaks in the 1300°C annealed sample.

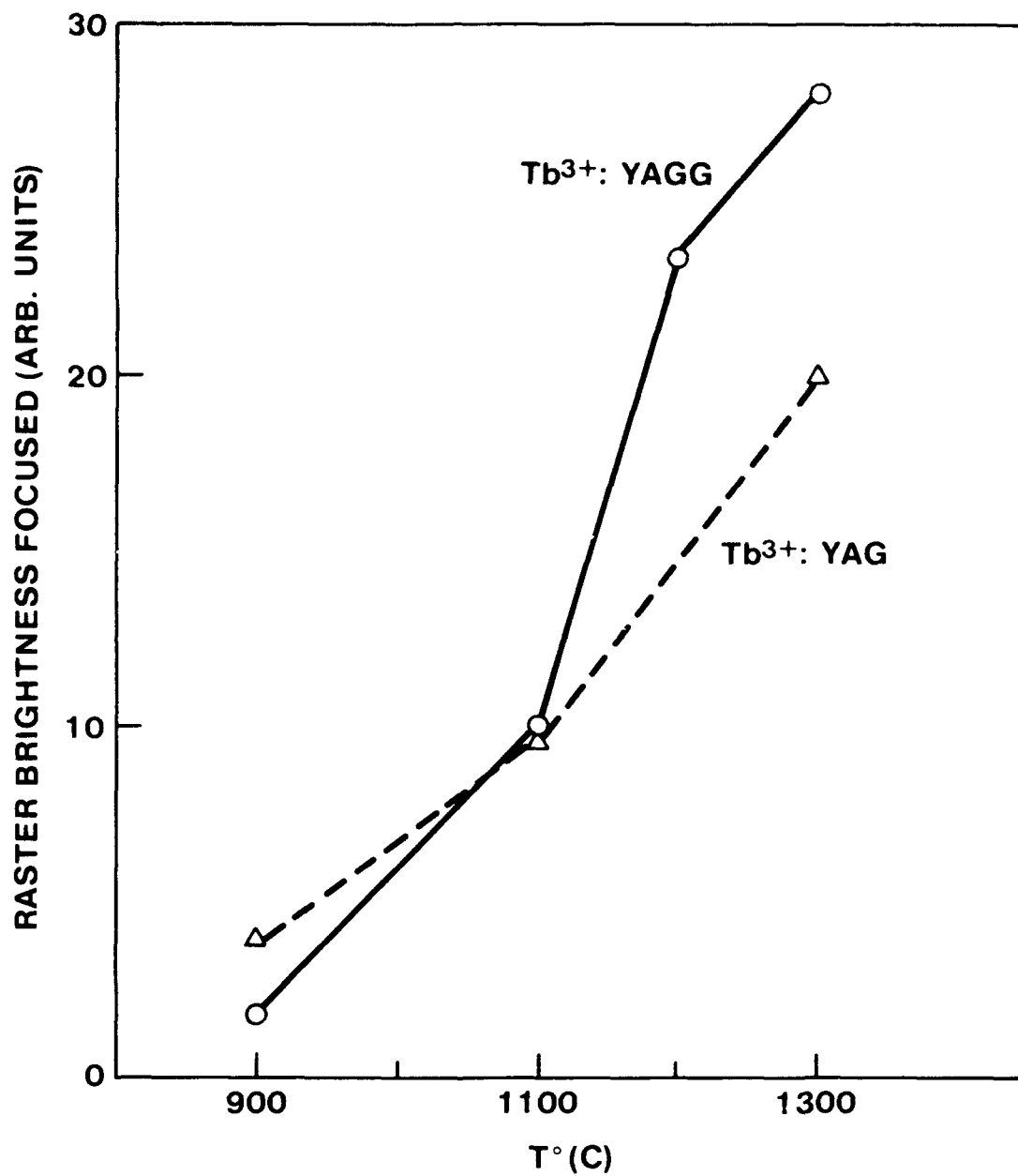


Figure 2 Relative raster brightness of typical sputtered $\text{Tb}^{3+}:\text{YAGG}$ and $\text{Tb}^{3+}:\text{YAG}$ films versus firing temperature at high power density excitation conditions. The acceleration potential of the e-beam is 15 kV.

hypothesis is supported by the fact, that a much smaller relative improvement is observed in Tb^{3+} :YAG, where no phase change is taking place, and the increase in brightness is associated only with grain growth and improved crystallinity of the phosphor.

TABLE 1. The relative performance of single crystal and sputtered Tb^{3+} : $\text{Y}_3\text{Al}_3\text{Ga}_2\text{O}_{12}$ and Tb^{3+} :YAG phosphors.⁽¹⁾

Phosphor	Form	$P_{\text{inst.}} = 10^4 \text{ w/m}^2$	$P_{\text{inst.}} = 10^{10} \text{ w/m}^2$	Deposition Conditions			
				$P_{\text{in.}} (\text{w})^{(2)}$	$[\text{O}_2] \%$	$P(\mu\text{m})^{(3)}$	$T_s (^\circ\text{C})^{(4)}$
Tb^{3+} : $\text{Y}_3\text{Al}_3\text{Ga}_2\text{O}_{12}$	Sputt.	2.16	2.04	250	9	22	180
"	"	2.21	2.01	150	9	25	210
"	"	2.21	1.84	150	17	50	310
"	"	2.25	2.06	250	17	44	180
Tb^{3+} :YAG ⁽⁵⁾	Sputt.	2.08	1.38	150	9	50	300
Tb^{3+} : $\text{Y}_3\text{Al}_3\text{Ga}_2\text{O}_{12}$ ⁽⁶⁾	Single Crys.	0.97	1.06				
Tb^{3+} :YAG ⁽⁶⁾	Single Crys.	0.93	0.62				

(1) The phosphors are excited by 15 kV e-beam. Sputtered films were fired at 1300°C for 2 hours. The results are normalized to the performance of Ce^{3+} : Tb^{3+} : $\text{Y}_3\text{Al}_3\text{Ga}_2\text{O}_{12}$ reference samples (see Ref. 1).

(2) Input power

(3) Total gas pressure

(4) Substrate holder temperature

(5) Data from ref. 1

(6) Data from ref. 10

The time-decay of emission from the luminescent $\text{Tb}^{3+}({}^5\text{D}_4)$ state in Tb^{3+} :YAGG samples fired at different temperatures is presented in Fig. 3. The Tb^{3+} ions are excited by an electron beam pulse of 50 μsec duration. The emission decay is exponential and the lifetime in Fig. 3 is calculated at 10% points. It is surprising in the view of a much smaller cathodoluminescent efficiency of the 900°C versus 1300°C fired films, that only a small difference in emitters lifetime is observed (see Fig. 3).

The surface morphology of a typical film annealed at 1300°C is shown in Fig. 4. The film is uniform and has a medium grain size of about 0.25 μm .

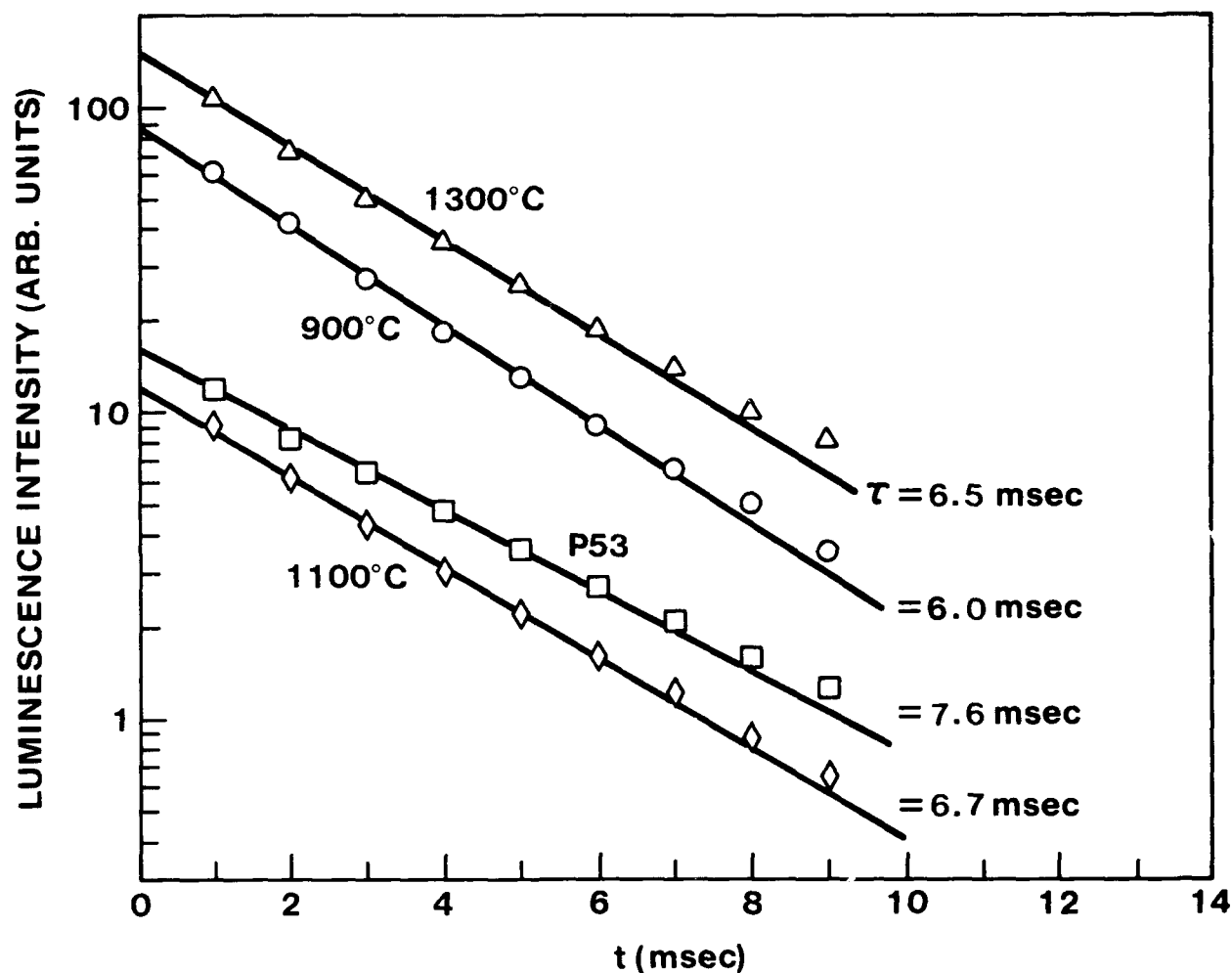


Figure 3 The decay of the $\text{Tb}^{3+}({}^5\text{D}_4)$ emission intensity versus time in sputtered Tb^{3+} :YAGG and commercial P53 phosphors following an e-beam excitation pulse of 50 μsec duration. The pulse repetition rate is 100 Hz, electron acceleration potential is 15 kV, and the beam is defocused to avoid possible saturation-related effects. The sputtered films were fired at the indicated temperatures for 2 hours in air.

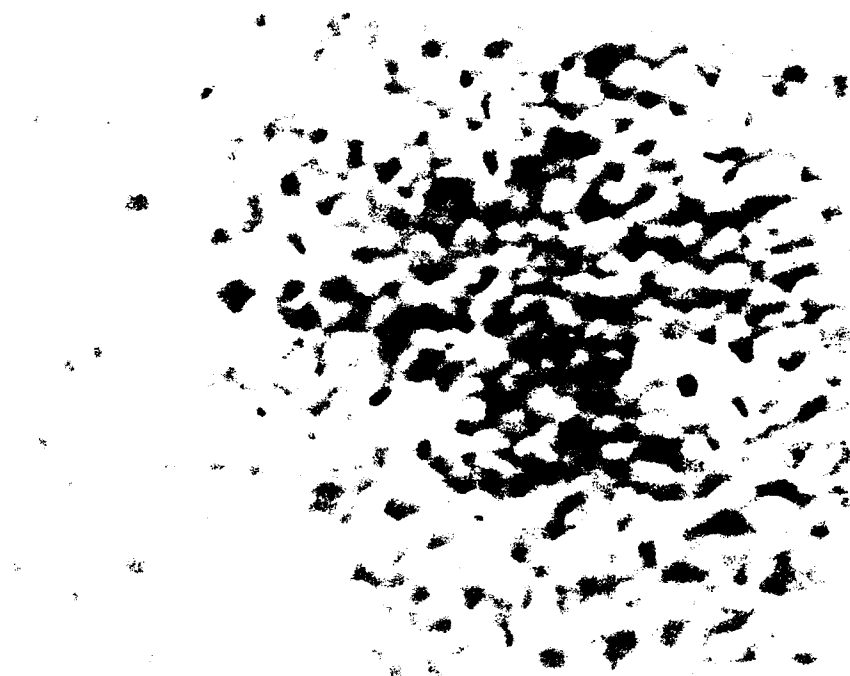


Figure 4 An SEM microphotograph of the surface of a sputtered Tb³⁺:YAGG film fired at 1300°C for 2 hours in air.

As in the case of Tb^{3+} :YAG films,^[1] we found that the deposition parameters are interrelated, and luminescent films with highest efficiency could be deposited using a variety of conditions, some of which are given in Table 1. In the same table we present data on single crystal Tb^{3+} :YAG and Tb^{3+} :YAGG films,^[10] as well as sputtered Tb^{3+} :YAG phosphors. Comparing the low power data from single crystal and from sputtered films, we note that Tb^{3+} :YAGG is as efficient in comparison to Tb^{3+} :YAG, as would be expected, based on the single crystal results (see Table 1). However, at the high power excitation conditions Tb^{3+} :YAGG is only 1.5 times brighter than Tb^{3+} :YAG, and not 1.7 times. A possible explanation of this result will be given below.

The composition of as-deposited and heat treated films was examined using the Rutherford Backscattering (RBS) technique. The results of evaluation of two films are given in Table 2. From Table 2 we see that the films are slightly yttrium and terbium rich. The deviation from the target composition is small, almost within the experimental error, however, very consistent. Loss of gallium after firing, observed in the first film, is not confirmed by the results from the second film. The oxygen concentration is stable in both films and close to stoichiometric.

TABLE 2. Atomic ratios of constituents in sputtered Tb^{3+} :YAGG films, as measured by RBS technique.⁽¹⁾

Sputtered Film	Atomic Ratios			
	Al/Y	Ga/Y	Tb/Y	O/Y
#1 — As Deposited	0.89	0.66	0.055	4.1
#1 — Fired 1300°C	0.89	0.63	0.055	3.9
#2 — As Deposited	1.0	0.65	0.059	4.0
#2 — Fired 1300°C	1.0	0.66	0.054	4.0
Target ⁽²⁾	1.05	0.70	0.053	4.2

- (1) An estimated instrumental error in measurements of Al/Y, Ga/Y, and Tb/Y ratios is 5%, and 15% in measurements of O/Y.
- (2) The target composition is $(\text{Y}_{2.85}\text{Tb}_{0.15})\text{Al}_3\text{Ga}_2\text{O}_{12}$.

To investigate any possible material loss during the heat treatment, two films were weighed before and after firing at 1300°C. The starting weights were 6.23 mg and 14.38 mg. After heat treatment the films lost 0.22 ± 0.10 mg and 0.23 ± 0.10 mg, respectively. Weight loss beyond the experimental error recorded in this experiment is believed to be due to Ga_2O_3 evaporation from the film, since the vapor pressure of this compound at the stated temperatures is much higher than that of Y_2O_3 and Al_2O_3 .^[12] We will address this result in the discussion below.

Two additional targets having the composition $(\text{Y}_{2.88}\text{Tb}_{0.12})\text{Al}_2\text{Ga}_3\text{O}_{12}$ and $(\text{Y}_{2.775}\text{Tb}_{0.225})\text{Al}_{2.7}\text{Ga}_{2.3}\text{O}_{12}$ were used to sputter films. In total about twenty runs were

performed with these targets. Although we did not find an increase in maximum light output, as compared to films described above, nevertheless, on the average, a 10% increase in brightness was observed. This is probably due to better reproducibility of these Ga^{3+} rich films in sputtering.

3. CRT Performance

A number of CRT's with 1-inch diameter sputtered $\text{Tb}^{3+}:\text{Y}_3\text{Al}_3\text{Ga}_2\text{O}_{12}$ faceplates have been fabricated. In Fig. 5 the performance of a CRT with a sputtered phosphor faceplate is compared to that of a state-of-the-art high brightness, high resolution CRT with a particulate P53 phosphor screen. The latter tube was developed recently by an outside vendor, and, as far as we know, is the best on the market. The sputtered tube was also manufactured by the same vendor, and both tubes have identical electron guns.

In Fig. 5 the peak line brightness and full width of the line at half maximum points (FWHM) are plotted versus screen current for the two tubes in consideration. Examining the data in Fig. 5, we see that the peak line brightness achievable with the sputtered faceplate does not fall off from that measured on a particulate screen at screen currents lower than 100 μA . At higher currents the sputtered phosphor saturates more rapidly and drops by 13% at 140 μA . At all currents the sputtered faceplate has a higher resolution, as is demonstrated by the FWHM data in Fig. 5. In addition, the spot size increases more rapidly with the screen current in the case of the particulate screen.

4. Discussion

The total gas pressure, oxygen concentration, and power density used in sputter-deposition of $\text{Tb}^{3+}:\text{Y}_3\text{Al}_3\text{Ga}_2\text{O}_{12}$ layers are similar to those used in preparation of $\text{Tb}^{3+}:\text{YAG}$ films. As in the latter case, heat treatment at high temperatures was a necessary step to achieve high cathodoluminescence efficiency (see Fig. 2). The most significant difference, however, in development of the above mentioned two compounds is the existence of high and low temperature phases in YAGG, that are not observed in YAG. From the x-ray diffraction data in Fig. 1 the lattice constant values for the low and high temperature phases are 12.173 Å and 12.085 Å, respectively. The change in lattice constant indicates a lattice contraction upon firing.

The observed lattice change can be explained by assuming that as-deposited the films are yttrium rich. This hypothesis is supported by RBS results indicating an excess of yttrium in the films. Assume that the sputtered films have a composition $(\text{Y}_{1-x-z}\text{Tb}_z)\text{Al}_{3-x-y}\text{Ga}_{2+y}\text{O}_{12}$ and the atomic ratios of Al/Y, Ga/Y, Tb/Y are 0.95, 0.65 and 0.055. The ratios are the average values from the results in Table 2, and we do not consider oxygen at this point because of rather large error in its concentration determination. It is easy to show that $x = 0.18$, $y = -0.04$, $z = 0.166$, in other words the composition $(\text{Y}_{0.814}\text{Tb}_{0.166})\text{Al}_{2.85}\text{Ga}_{1.96}\text{O}_{12}$, will satisfy the RBS results.

Since Tb^{3+} ions are too large to fit anywhere except the dodecahedral sites, it means that 0.18 ions of Y^{3+} are on the octahedral sites, usually occupied by Al^{3+} or Ga^{3+} ions.^[12] The ionic radius of Y^{3+} is 0.892 Å, as compared to 0.62 Å and 0.53 Å for Ga^{3+} and Al^{3+} , respectively.^[13] Substitution of Y^{3+} for Ga^{3+} or Al^{3+} will expand the lattice. Based on the composition derived above, one calculates the lattice constant of the film to be 12.150 Å.^[12-14] Considering the fact that the RBS is a surface analysis technique and does not provide information about the bulk of the film, there is a degree of uncertainty in the composition of the film used in the calculations. In these circumstances the agreement between the observed (12.173 Å) and calculated lattice constants can be considered satisfactory.

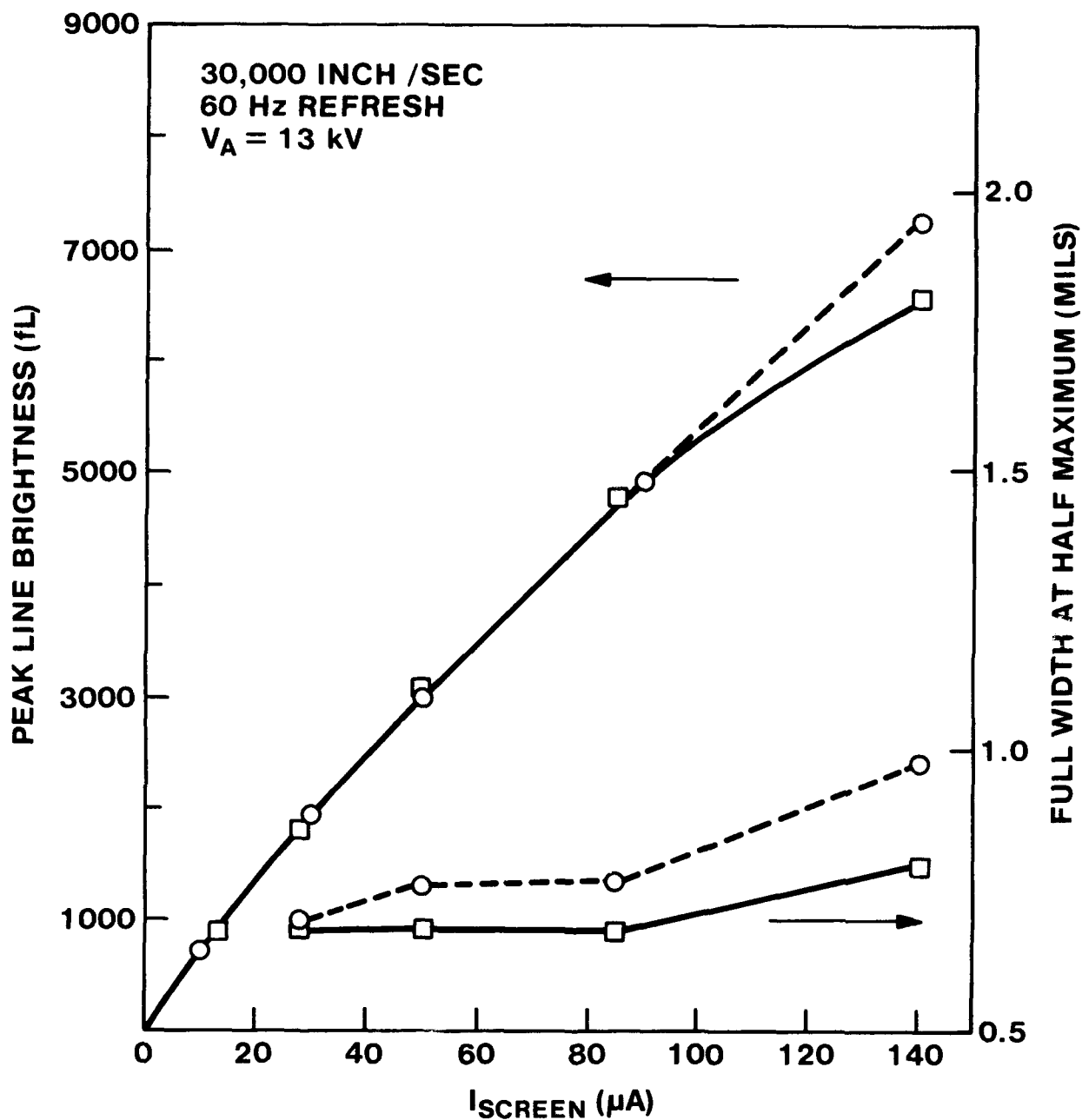


Figure 5 The peak line brightness and the full linewidth at half-maximum points (FWHM) measured on a commercial P53 and sputtered Tb^{3+} :YAGG phosphors faceplates versus screen current. The e-beam is focused and is scanning in a stroke mode. □ — an optimized sputtered Tb^{3+} :YAGG phosphor; ○ — commercial P53. Both CRT's have the same electron guns.

To explain consistently the observed contraction of the lattice upon heat treatment, we have to assume Al^{3+} diffusion from the substrate into the film following Ga_2O_3 evaporation. The increase of Al^{3+} concentration in the layer decreases the lattice constant, because it substitutes for larger Y^{3+} and Ga^{3+} ions on the octahedral sites. Any uncompensated loss of Ga^{3+} will increase the amount of Y^{3+} on the octahedral sites in order to preserve the garnet structure, which will expand the lattice even further. Theoretically, if the excess Y^{3+} ions diffuse into the substrate, it will also decrease the lattice constant of the film. However, an RBS analysis of the substrate, from which a fired film was etched off, revealed only small amounts of Ga^{3+} in the top 200 Å layer.

In an alternative approach one can assume a stoichiometric film composition $(\text{YTb})_3(\text{AlGa})_5\text{O}_{12}$ before and after firing. Based on the lattice constants' data obtained with pure aluminum and gallium garnets,^[12] the experimentally-observed lattice constants correspond to the following film composition for the low and high temperature phases respectively: $(\text{YTb})_3\text{Al}_{1.8}\text{Ga}_{3.2}\text{O}_{12}$ and $(\text{YTb})_3\text{Al}_{3.34}\text{Ga}_{1.66}\text{O}_{12}$. Here too, the lattice contraction is explained by an increase in Al^{3+} ion concentration in the film.

We have an experimental proof of a reaction between the Al_2O_3 substrate and the $\text{Tb}^{3+}:\text{YAGG}$ film. A polished sapphire substrate on which a $\text{Tb}^{3+}:\text{YAGG}$ film was deposited, annealed at 1300°C and then etched off, showed surface roughness of an order of 200 Å. This was not observed in the substrate areas masked during film deposition. Unfortunately, it is difficult to say from this experiment how many Al^{3+} ions diffused into the deposited layer.

The weight loss recorded after the heat treatment supports the hypothesis of an yttrium rich rather than of a stoichiometric film. In a stoichiometric film a substitution of 1.54Ga^{3+} ions per garnet molecule by Al^{3+} (see above) should manifest itself in a 16% weight loss, whereas a loss of 3.5% and 1.7% was observed experimentally.

From the other side, only 0.66 Al^{3+} ions per garnet molecule have to be added and 0.33Ga^{3+} ions removed to convert the $(\text{Y}_{3.014}\text{Tb}_{0.166})\text{Al}_{2.86}\text{Ga}_{1.96}\text{O}_{12}$ film to $(\text{Y}_{2.84}\text{Tb}_{0.16})\text{Al}_{3.34}\text{Ga}_{1.66}\text{O}_{12}$, having the desired lattice constant. The expected weight loss in this case should be 3.6%, in good agreement with the experiment. The fact that the measured weight loss is not proportional to the total weight of the film, but is rather independent of it, suggests that the Ga_2O_3 evaporation takes place from the surface only. Its rate is controlled by the Ga^{3+} diffusion to the surface and for a certain amount of time does not depend on the total mass of the film.

The observed features of the temperature and time dependent transformation of the low temperature phase into the high temperature one find their logical explanation in the Al^{3+} for Ga^{3+} substitution governed by the diffusion processes. Below 1100°C the diffusion is apparently slow, and the film's composition is close to as-deposited, which is probably an yttrium rich garnet (see Figure 1). At 1100°C we start to see the appearance of both phases. As the firing temperature rises, more Al^{3+} ions diffuse into the film during the soaking period, and a larger portion of the film becomes stoichiometric. This explains the growth of the high temperature phase at the expense of the low temperature phase. At 1300°C the process is fast enough that during the firing period the transformation is completed, and only the high temperature phase is observed. A direct measurement of Y^{3+} , Al^{3+} , and Ga^{3+} concentrations in the film as a function of depth after various heat treatments is needed to prove the proposed model.

The results in Table 1 clearly show that in a sputtered $\text{Tb}^{3+}:\text{YAGG}$ material we achieve an internal conversion efficiency equal to that of a single crystal phosphor of the same composition. At high power excitation, the sputtered $\text{Tb}^{3+}:\text{Y}_3\text{Al}_3\text{Ga}_2\text{O}_{12}$ film reaches 88% of

the brightness value anticipated based on the brightness of the sputtered $\text{Tb}^{3+}\text{:YAG}$, if we assume that the respective brightnesses in sputtered films will scale according to the single crystal results. In a recent paper, K. Ohno and T. Abe^[15] published the results of their study of $\text{Tb}^{3+}\text{:Y}_3(\text{AlGa})_5\text{O}_{12}$ powder phosphors. They found that the optimum composition for high power excitation conditions is $\text{Tb}^{3+}\text{:Y}_3\text{Al}_2\text{Ga}_3\text{O}_{12}$, and not $\text{Tb}^{3+}\text{:Y}_3\text{Al}_3\text{Ga}_2\text{O}_{12}$. However, both phosphors have the same efficiency at low power excitation. If we do lose Ga_2O_3 during heat treatment, the sputtered film will saturate quicker than is anticipated for a composition with two gallium ions per garnet molecule. On the other hand, this will not affect the low power excitation results. More, in light of Ohno and Abe results, we would expect to gain at high current densities and to be able to match in peak line brightness the commercial P53 at all currents (see Fig. 5) by increasing the amount of gallium in the target and, therefore, in the film. However, our experiments with Ga^{3+} rich films did not support this expectation. We did not prepare films of higher brightness, but rather of better reproducibility, by increasing the amount of Ga^{3+} in the film.

If the sputtered phosphor is assumed to be in full optical contact with the substrate and the powder phosphor with no optical contact, at equal conversion efficiencies the brightness of the latter should be n^2 times higher,^[11] where n is the refractive index of the substrate. For sapphire $n^2 = 3.1$. The fact that the observed peak line brightnesses of the sputtered and particulate phosphors are the same in a broad current range (see Fig. 5) cannot be explained by a smaller spot size in the first case*, and requires additional explanation.

The brightness ratio between the identical powder and sputtered phosphors can be much closer to unity than predicted above, if: a) a partial optical contact exists between the powder phosphor layer and the faceplate; b) the sputtered layer is not in full optical contact with the substrate; c) the sputtered film has a higher internal conversion efficiency; d) insufficient heat dissipation by the powder phosphor layer causes a temperature rise and an associated thermal quenching of the luminescence. Let us discuss the influence of the above mentioned factors in a little more detail.

- a,b). It was shown by Kapany^[9] that neither sputtered nor powder layers are in full contact or with no contact, respectively, with the faceplate. Therefore, one should anticipate to measure a smaller than n^2 brightness ratio, probably around $0.7n^2$.
- c). It is essential to use small grain particulate phosphors in high resolution screens. On the other hand, it is known that small grain phosphors usually have a lower conversion efficiency. The sputtered film has a conversion efficiency equal to that of the single crystal, and probably higher than the powder phosphor.
- d). To estimate the rise in temperature of the powder phosphor layer at given excitation conditions is usually very difficult, because the thermal conductivity of the layer is not known. The thermal conductivity is a function of the grain size, screen density, and deposition technique. To the best of our knowledge, there are no experimental or theoretical data published concerning this parameter.

As we see, it is very difficult to predict which of the above mentioned factors is critical. Most probably they all contribute to some extent to the observed result, and their importance changes depending on the specific conditions of the experiment. However, regardless of the

* Based on the data in Fig. 5 we are talking about a 20% increase in brightness due to a smaller spot size.

relative influence of the different discussed parameters on the light output from the sputtered and particulate screens, the sputtered phosphors proved to be a serious competitor to the finest conventional powder screens available.

The advantages of thin films could become especially important in small-size high-resolution color CRT's. For example, resolution unachievable with conventional technology could be demonstrated using a multilayer screen of a penetration type. Also, in a single layer screen approach a thin film phosphor allows patterning with a much higher resolution than a powder phosphor.

III. OPTICAL ISOLATION STRUCTURE

I. Introduction

As mentioned in Section II, thin translucent films in optical contact with the substrate will suffer a loss in light output in comparison to a powder phosphor of the same internal efficiency. The latter phosphor is assumed not to be in optical contact with the substrate. This limitation is fundamental, and to increase the light output from a film in optical contact with the substrate, substrates of lower refractive index should be used. Unfortunately, there are very few materials that have a low refractive index and can withstand the high processing temperatures currently necessary for preparation of efficient sputtered phosphor layers.

The only substrate material available to us that satisfies the temperature and refractive index requirements is silica, SiO_2 . It has one of the lowest refractive indexes ($n = 1.46$) among solids and would allow processing at elevated temperatures (up to about 1250°C). The major disadvantage of this material is a very low thermal expansion coefficient $0.5 \times 10^{-6} \text{ }^\circ\text{K}^{-1}$, as compared to about $7 \times 10^{-6} \text{ }^\circ\text{K}^{-1}$ for garnets. It would be impossible to deposit a garnet film on SiO_2 substrate and to anneal it to required temperatures without cracking the film. Our experiments with YAGG films on SiO_2 confirmed this prediction.

On the other hand,^[16] it is known from mechanics, that a thinner film of material deposited on a substrate with a substantially different thermal expansion coefficient could be heated without damage to higher temperatures than a thicker film. From an optics point of view, only the medium at about one wavelength depth from the emitting phosphor layer is of importance, since it defines the angular distribution of the transmitted light. The light distribution within the translucent phosphor layer is Lambertian and we assume that it is preserved within the substrate. Therefore, by depositing a thin layer of low refractive index material at the phosphor/substrate interface, we create a Lambertian source of equal intensity in the low refractive index medium (See Figure 6). The further propagation of light through the transparent substrate structure that could be composed from more than one material is defined only by the refractive index of the layer adjacent to the phosphor layer. With this arrangement, the amount of light collected by an outside observer will be increased by $(n_s/n_f)^2$, where n_s and n_f are the refractive indexes of the substrate material without the isolation film and of the film itself, respectively. In the case of a SiO_2 layer on sapphire, the expected gain in light output is 45% ($n_s = 1.76$; $n_f = 1.46$).

The predicted increase in light output does not violate the brightness conservation law of optics.^[17] The additional light is collected due to re-scattering at the phosphor/film interface, which leads to a lateral diffusion of light in the phosphor layer and to an increase in spot size. However, the light diffusion length is of the order of the scattering layer thickness^[18] and is negligible in most applications. If the viewer cannot resolve the change in the spot size, the increased light flux is perceived as an increase in brightness. Clearly, no gain in intensi-

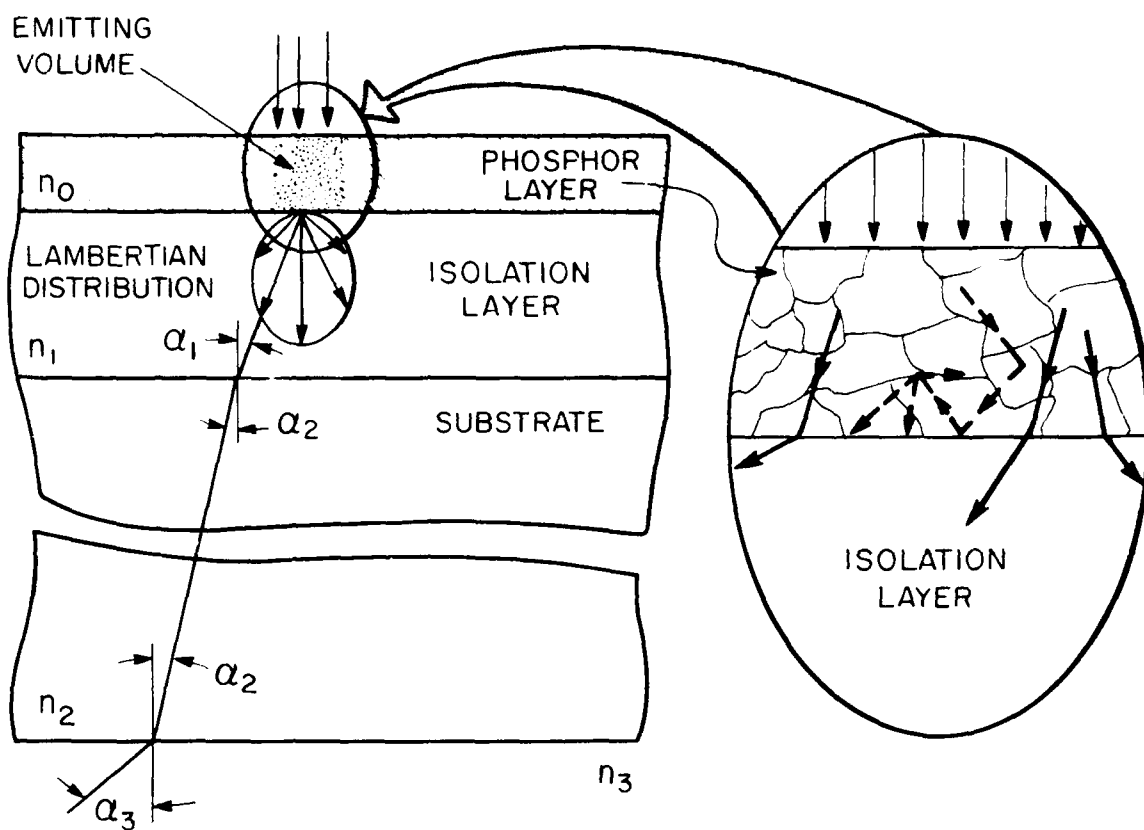


Figure 6 A schematic presentation of an optical isolation structure for CRT screens. n_0 , n_1 , n_2 , and n_3 are the refractive indexes of the phosphor layer, the isolation layer, the substrate, and the output medium, respectively. It is assumed here, that $n_1 < n_0$, and $n_1 < n_2$, therefore $\alpha_1 > \alpha_2$.

could be achieved by depositing a transparent phosphor layer on any transparent substrate, since without a scattering mechanism an increase in image brightness would contradict the brightness conservation law.

In the rest of this section we will describe our experiments toward fabricating a thin film phosphor faceplate with SiO_2 isolation layers.

2. Experimental Results and Discussion

Most of our SiO_2 layers were prepared by the Low Pressure Chemical Vapor Deposition (LPCVD) technique from tetrathyl orthosilicate (TEOS) precursors. Silica films from 5000 Å to 10,000 Å thick were deposited at 700°C on one-inch-diameter sapphire substrates. In some cases the layers were doped with phosphorus in amounts of 2 to 8%. Doping with phosphorus reduces the softening temperature of the glass and would be expected to reduce the stress in the film during annealing.

Initial experiments were conducted with SiO_2 layers on sapphire without the P53 layer. We found that 5000 Å thick films of SiO_2 on sapphire could be soaked for 2 hours to 1300°C without any apparent changes in the films' state. The films stayed transparent without visible cracks. X-ray powder diffraction measurements revealed that up to 1250°C there is no formation of a cristobalite phase. In samples annealed at 1300°C we do detect traces of cristobalite, but the crystals are small enough not to affect the visual appearance of the film. Thicker films would occasionally develop a hazy appearance after annealing at 1300°C. This is to be expected, since larger grains could grow easier in thicker films. Nevertheless, a number of 10,000 Å thick silica films went through the 1300°C annealing without any visible changes. Phosphorus doped films did not promote visible cristobalite growth up to 1300°C. It is known that phosphorus addition retards crystallization. To summarize, our experiments showed that SiO_2 films up to 1-μm thick deposited on sapphire could be heated to 1300°C and retain their good optical quality. In our opinion this is a very significant and encouraging result.

After verifying that SiO_2 films would cycle to required temperatures, the next step was to deposit a phosphor layer on top of the silica film and to anneal the structure. Tb^{3+} :YAGG films of about 2 μm thick were deposited and annealed in the temperature range from 900°C to 1300°C. The heat treatment was in air as described in Section II.

Phosphor films annealed up to 1100°C showed very good adhesion. However, no increase in luminescence was observed, because the garnet film remained transparent. As we explained above, no increase in light output could be gained from the structure with transparent phosphor films.

Films annealed at temperatures above 1200°C developed various problems. They blistered, cracked, or peeled, and sometimes had all the above problems simultaneously. A microphotograph of a typical YAGG film deposited on a 5000 Å SiO_2 layer on sapphire is shown in Figure 7. A blistering and cracking of the film is clearly visible. We also found that at this temperature the YAGG films react with silica, which represents a more fundamental problem. The surface morphology of a thin 1000 Å Tb^{3+} :YAGG film deposited on top of a 5000 Å SiO_2 film annealed at 1250°C is shown in Figure 8. A surface roughness on a much larger than 1000 Å scale is a clear indication of a reaction that took place between the layers in this experiment.

The main product of the YAGG and SiO_2 reaction was identified to be $\text{Y}_2\text{Si}_2\text{O}_7$ by using X-ray powder diffractometry. The X-ray diffraction spectra of a Tb^{3+} :YAGG film on sapphire and on a 5000 Å thick SiO_2 film are compared in Figure 9. A reference spectrum of $\text{Y}_2\text{Si}_2\text{O}_7$ is also shown in Figure 9 for comparison.



Figure 7 An optical micrograph of a 1.5 μm thick Tb^{3+} :YAGG film deposited on 5000 \AA SiO_2 film on sapphire. The sample was annealed in air at 1250°C for 2 hours.

Figure 8 An S.E.M micrograph of a thin (1000 \AA) Tb^{3+} :YAGG film deposited on 5000 \AA SiO_2 layer on sapphire. Sample was annealed for 2 hours at 1250°C in air.

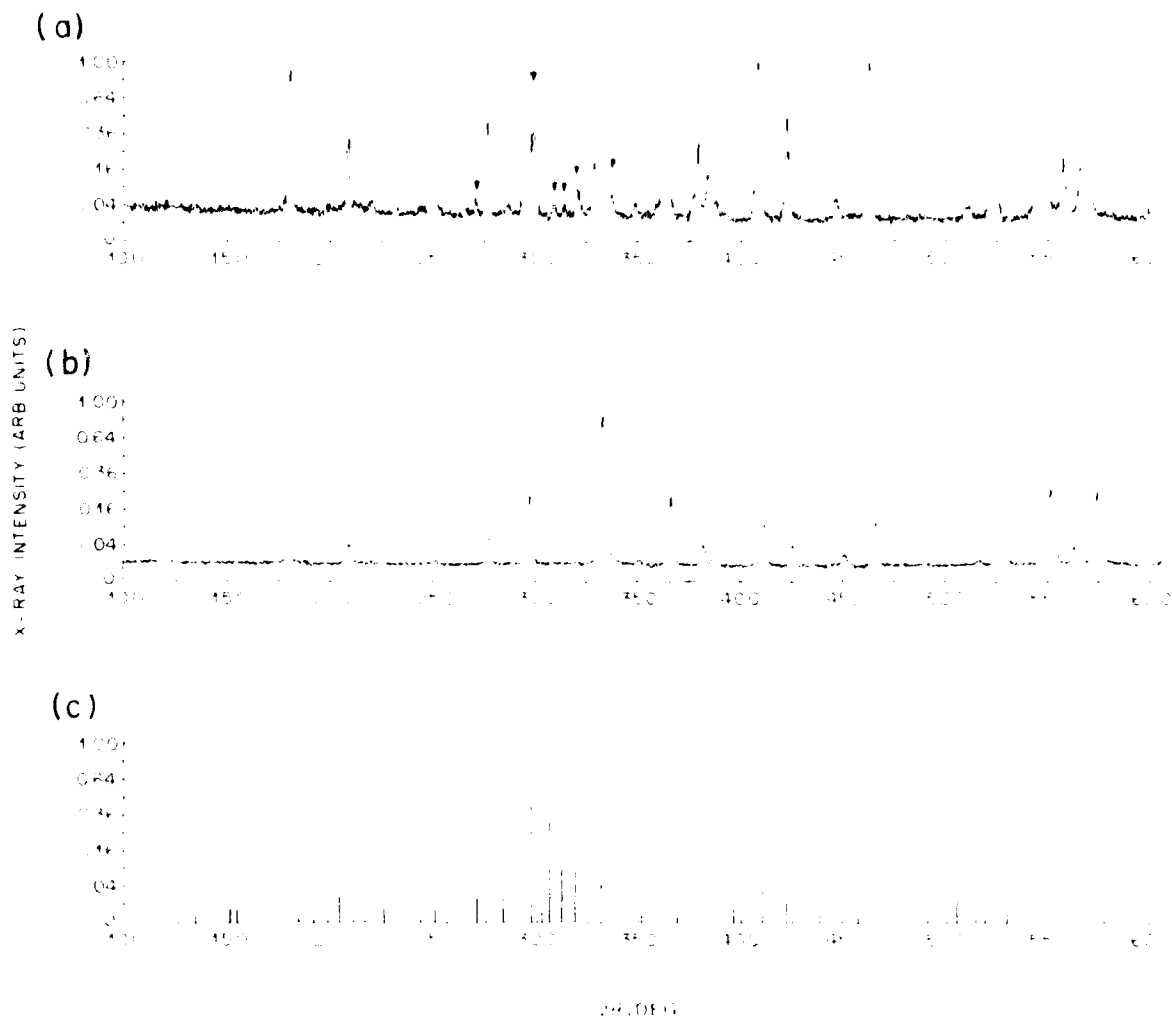


Figure 9 X-ray powder diffraction spectra of a 1.5 μm thick Tb^{3+} :YAGG film deposited onto: a) 5000 Å SiO_2 layer on sapphire; b) on sapphire. Both samples were annealed in air at 1300°C for 2 hours. The arrows mark $\text{Y}_2\text{Si}_2\text{O}_7$ lines, according to the reference pattern #21-1457 [23] given in c).

The $\text{Y}_2\text{Si}_2\text{O}_7$ lines observed in Figure 9 are relatively weak in comparison to YAGG lines, and the overall YAGG line structure is preserved. The spectrum changes completely when a phosphor film is deposited on a 10,000 Å silica film and annealed to 1300°C. Larger amounts of SiO_2 available for the reaction suppress the YAGG spectrum (see Figure 10a). In the resultant spectrum, in addition to $\text{Y}_2\text{Si}_2\text{O}_7$ lines, we now identify lines of Al_2SiO_5 . Both $\text{Y}_2\text{Si}_2\text{O}_7$ and YAGG are dissolved in hot phosphoric acid much faster than Al_2SiO_5 , and after etching the sample in hot H_3PO_4 , the dominant spectrum observed is that of Al_2SiO_5 (see Figure 10b). The light output from the films on SiO_2 layers was typically lower than that from a reference film deposited directly on sapphire and annealed at the same conditions. Reaction between the layers, as we see, adversely affects the efficiency of the phosphor layer.

Films deposited on phosphorus doped silica layers typically showed better adhesion than that observed in the same conditions on an undoped SiO_2 layer. However, they also reacted with the silica layer and showed poor luminescence.

After it became clear that a reaction is taking place between the garnet and SiO_2 layers, it was natural to try to find a transparent barrier layer to prevent the reaction between the phosphor and SiO_2 . A number of barrier layers were tried: Al_2O_3 , ZrO_2 , BN, and Si_3N_4 . ZrO_2 and Si_3N_4 were prepared by a reactive e-beam evaporation; BN was prepared by CVD (chemical vapor deposition); Al_2O_3 was deposited by reactive e-beam evaporation and sputtering; Si_3N_4 was deposited by Plasma Enhanced Chemical Vapor Deposition (PECVD). Film thicknesses as high as 2000 Å were used. None of these layers worked as a barrier for YAGG at 1300°C, although no reaction was observed between the above mentioned barrier layers and the SiO_2 up to 1300°C, and the films remained transparent. Use of thicker barrier layers would defeat the purpose of this structure, since they typically have a high refractive index. It is interesting to note that no reaction was observed between the SiO_2 and Al_2O_3 layers, whereas we know one of the crystal phases formed in the YAGG and SiO_2 reaction is Al_2SiO_5 . Apparently, presence of yttrium or gallium promotes Al_2SiO_5 formation.

In our experiments with barrier materials most of our attention was devoted to Al_2O_3 , since good results on YAGG deposition were obtained with sapphire substrates. The layers were deposited by RF-sputtering from a single crystal sapphire target, or by reactive evaporation of Al. It is known, that vacuum deposited Al_2O_3 layers densify upon annealing at 800°C-1000°C.^[19] In our case, the etch rate of as-sputtered Al_2O_3 film in H_3PO_4 heated to 40°C dropped from about 300 Å/min to almost zero, upon annealing for 2 hours at 1000°C. Nevertheless, the densified Al_2O_3 layer did not prevent reaction at the garnet/ SiO_2 interface.

In total more than 70 samples exploring various combinations of SiO_2 and barrier layers were tried, however in most cases the light output was lower than that obtainable with a reference film on a sapphire sample prepared and annealed in the same conditions. In a number of cases we did see an expected increase in light output, but could not repeat the results. The approach of optical isolation of the luminescent film from the substrate did not materialize due to the high reactivity of the garnet layers at elevated processing temperatures.

IV. ANTI-HALO FILTER FOR THIN-FILM PHOSPHORS

In every CRT screen the phosphor layer is in partial optical contact with the faceplate, so there are rays that travel at large incident angles to the surface of the faceplate. Due to total internal reflection such rays are trapped, and upon reflection at the front surface are scattered by the phosphor, giving rise to a "halo" pattern. J. Rancourt^[20] proposed to use a multilayer interference edge-filter to reduce the problem. An edge-filter is a filter that in a narrow wavelength interval will transmit the rays that fall on it at angles smaller than a certain limiting

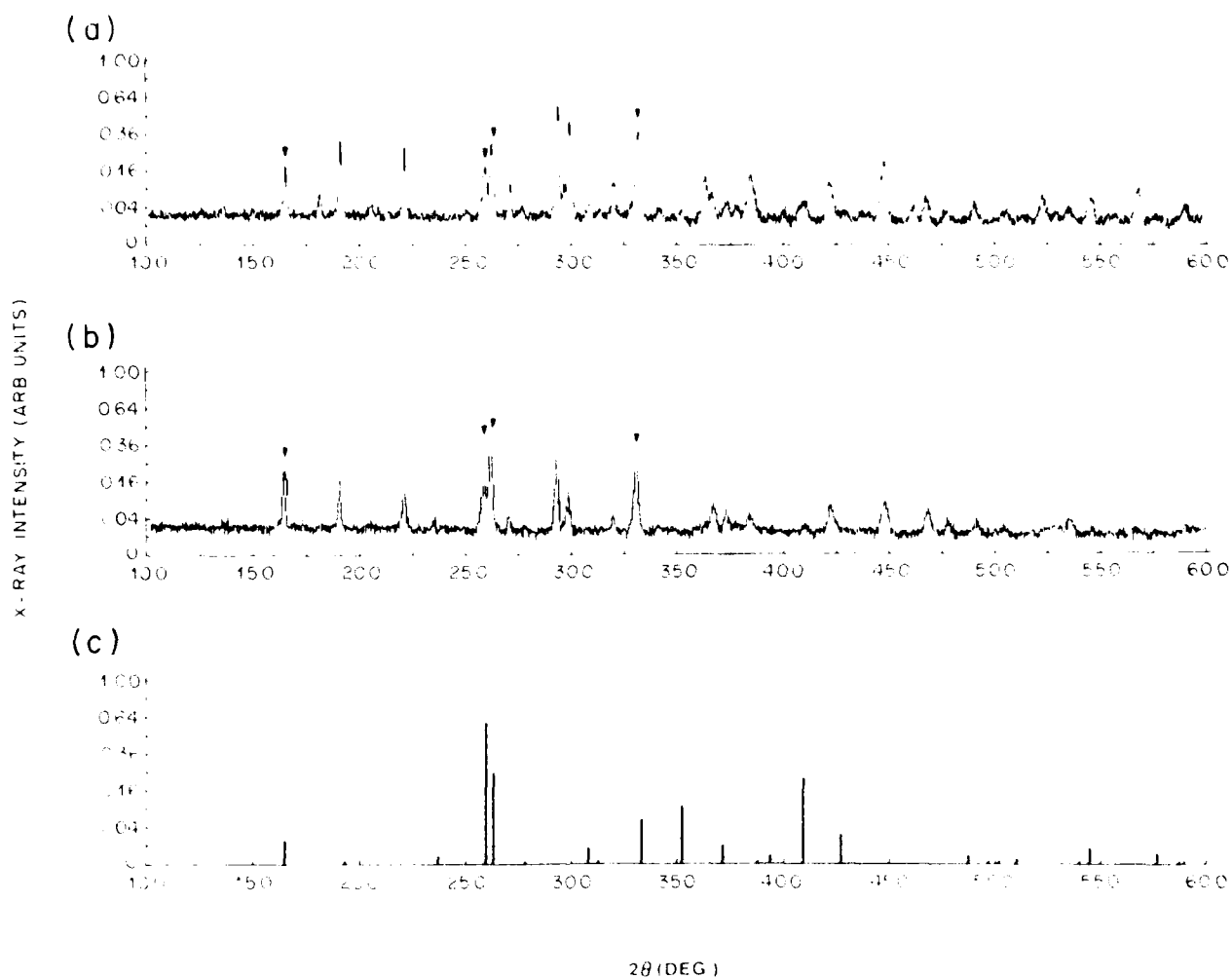


Figure 10 a) X-ray powder diffraction spectra of a 1.5 μm thick Tb^{3+} :YAGG film deposited onto 10,000 Å SiO_2 layer on sapphire and annealed in air at 1300°C for 2 hours; b) The same, after a 6 min etch in an un-diluted H_3PO_4 (200°C). The arrows mark Al_2SiO_5 lines, according to the reference pattern #22-18 [23] given in c).

angle, and will reflect the rest. Such a filter prevents the rays traveling at large angles from entering the faceplate and forces them to scatter at the phosphor layer. Moreover, the rays that would not be normally trapped in the faceplate, but still would propagate at large angles, are typically not collected by an imaging system. By forcing them to re-scatter, a large fraction of them will be emitted at lower angles, thereby increasing the light flux from the spot.

An edge-filter is particularly beneficial in applications where thin film phosphors are used. It had been shown that the diffusion length for light diffusing laterally in the phosphor layer is of the order of the layer thickness.^[18] Sputtered films are dense, and typically a 1 μm film will effectively absorb the incoming energy of a 15 kV beam.^[21] Therefore, with thin films lateral light diffusion will not significantly degrade the spot size for a majority of applications, and will be much smaller than that expected with powder phosphor layer. Since only rays in a narrow cone around the normal to the surface of the faceplate will propagate, it eliminates the light trapping and associated contrast problems.

This idea is very similar to the one we presented for the isolation layer. The difference is that this approach is applicable only to narrow band-width emitters, whereas the isolation layer could be used with any phosphor. However, the edge-filter approach will concentrate light into a narrower cone, and by virtue of this, increase the light flux in the forward direction more than that obtainable with isolation layers.

Based on this reasoning, we contracted an outside vendor to prepare for us edge-filter coatings on sapphire that would be designed for Tb^{3+} emission and would withstand the heating cycle. The contract was divided into two stages. During the first stage, two sets of multilayer filters from different materials would be prepared in approximate thicknesses to check their compatibility with high temperature processing. If the deposited filters would pass successfully through the annealing test, they would be sent to us for phosphor layer deposition. After deposition and successful annealing of the films, stage two of the contract would be activated. Here, accurately calibrated filters would be deposited by the vendor and sent to us for phosphor deposition and incorporation into CRT's.

The program, unfortunately, did not advance beyond the first stage, since the filter layers reacted between themselves, and the filter lost its properties (a report from the vendor is attached in the Appendix). As a result of our experience with the stage I of the contract, the vendor did not recommended proceeding with stage II. They estimated that the chance for success was too low with the current temperature cycling requirements. Following their recommendation, we stopped the program at this point.

V. CONCLUSION

The subject of this contract was high brightness, high-resolution military CRT's. It started as work on single crystal phosphors (see previous reports under this contract), and at the later stages evolved into a study of thin film poly-crystalline phosphors. One could arbitrarily divide the development of poly-crystalline thin film phosphor screens for CRT applications into two stages. Success with both would ensure thin film phosphor's use in a wide range of CRT's. The goal of stage one would be to learn to deposit efficient and stable phosphor layers by thin film technique. In work under this contract we have demonstrated successful deposition of $\text{Tb}^{3+}:\text{YAG}^{[1]}$ and $\text{Tb}^{3+}:\text{Y}_3\text{Al}_3\text{Ga}_2\text{O}_{12}$ thin film phosphors by the RF-sputtering technique. Internal conversion efficiency matching that of the single crystal phosphor was achieved. In a line-scan condition the peak line brightness observed on the sputtered P53 phosphor screen is equal to or only slightly lower than that achievable with a state-of-the-art

powder P53 phosphor screen, but offers a considerably higher resolution. P53 is one of the best green phosphors available to-date. By showing ability to deposit it by sputtering, we effectively accomplished the first stage.

The second stage of the thin film implementation process should concentrate on the solution of the optical contact problem. With transparent phosphor/substrate structures the escaping light flux is uniquely defined by the refractive index of the phosphor layer, as follows from the brightness conservation law, and cannot be increased. With translucent phosphor films, due to the scattering nature of the film, we can increase the collected light flux by trading off some resolution. Two approaches were tried in this work: the first is the optical isolation structure; the second is the anti-halo filter. In both cases we were not able to surpass the brightness that was achieved on a plain sapphire substrate, but nevertheless important information was gained from these experiments. We have shown that 10,000 Å SiO_2 films on sapphire could withstand heating to 1300°C. We have also learned that up to 1100°C interference filters deposited by our vendor retained their properties and P53 phosphor layers did not react with the silica film.

At higher temperatures SiO_2 reacted with the Tb^{3+} :YAGG layer, and layers composing the interference filter reacted between themselves. In our opinion, the next step toward the solution of the optical contact problems should be lowering of the process temperature to about (1000-1100)°C. In this range, as our current results indicate, a large degree of confidence exists that both light extraction schemes discussed here would work. A way to achieve a lower processing temperature is to deposit the film in a crystalline form in vacuum, utilizing the high surface mobility of the arriving atoms. The data presented in Ref. 23 describes single crystal garnet layers that were sputter deposited at 600°C. Those were not luminescent layers, nevertheless we feel that this results support the feasibility of efficient thin film phosphor deposition at lower temperature. It is obvious that if another phosphor would be found that does not require such high processing temperatures as garnets currently need, it would be already possible to successfully implement the phosphor/substrate decoupling schemes discussed above.

REFERENCES

1. J. Shmulovich and L. Luther, Air Force report under contract No. F33615-84-C-0503 for the period Jan. 8, 1986 - Jan. 15, 1987.
2. A. Pfahnl, Bell Sys. Tech. J. **42**, 181 (1963).
3. C. Infante, Int. Symp. Soc. Inf. Display, Seminar Lecture Notes, Orlando, FL, **1**, 1 (1985).
4. H. Yamamoto, H. Matsukiyo, T. Suzuki, and O. Kanehisa, Int.Symp. Soc. Inf. Display, Digest Tech. Papers, **16**, 51 (1985).
5. B. R. Critchley and J. Lunt, Int. Symp. Soc. Inf. Display, Digest Tech. Papers, Philadelphia, PA, **14**, 122 (1983).
6. T. E. Peters, J. Electrochem. Soc. **116**(7), 985 (1969).
7. N. Tsuda, M. Tamatani, and T. Sato, Extended Abstracts, Fall Meeting Electrochemical Soc. New Orleans, LA, 1984, p. 867.
8. "Optical Characteristics of Cathode Ray Tube Screens", Electronic Industries Assoc., TEPAC Publication No. 116, Dec. 1980.
9. N. S. Kapany, "Fiber Optics", Academic Press, New York, N.Y., 1967.
10. J. Shmulovich, G. W. Berkstresser, and G. Matulis, Extended Abstracts, Fall Meet. Electrochem. Soc., San Diego, CA, 1986, p. 1030.
11. W. Pickarczyk and A. Pajaczowska, J. Crystal Growth, **46**, 483 (1979); "Handbook of Chemistry and Physics", CRC Press, 63rd ed. (1982-1983).
12. S. Geller, Zeitschrift für Kristallographic, **125**, S.1 (1967).
13. R. D. Shannon and C. T. Prewitt, Acta Cryst. **B25**, 925 (1970).
14. C. D. Brandle and R. L. Barns, J. Crystal Growth, **26**, 169 (1974).
15. K. Ohno and T. Abe, J. Electrochem. Soc. **134**(8), 2072 (1987).
16. E. Suhir, ASME J. Applied Mechanics, **110**, 143 (1988).
17. M. V. Klein, "Optics", John Wiley & Sons, New York, 1970.
18. W. Busselt, R. Rane, J. Electrochem. Sec. **135**(3), 764 (1988).
19. J. A. Aboaf, J. Electrochem Soc. **114**(9), 948 (1967).
20. J. Rancourt, Int. Symp. Soc. Inf. Display, Digest Tech. Papers, Philadelphia, PA, **14**, 22 (1983).
21. T. E. Everhart and P. H. Hoff, J. Applied Aphys. **42**(13), 5837 (1971).
22. T. Takayama, K. Takaki and T. Kobayashi, Jap. Patent Appl. No. 61-15620, Jan. 29, 1986.
23. Powder Diffraction File, published by Joint Committee on Powder Diffraction Standards, Philadelphia, PA, August 1967.

APPENDIX

High Temperature Coatings for Use with Sputtered CRT Phosphors. Work done for Bell Laboratories, April, 1988.

INTRODUCTION

The goal of this effort was to produce a coating which is beyond the current state of the art, since coatings which meet the requested performance goals are not readily available. Specifically, the coatings had to survive a high temperature bake of 1300°C. The substrate material which can withstand this temperature is aluminum oxide (melting point 2040°C, whereas silica melts at 1600°C).

We recognized from the beginning that this temperature regime is not a standard environment for thin film coatings, and so we undertook the effort with the understanding that the initial samples that we would prepare would evaluate the temperature stability of the coatings. In addition, we planned to use new proprietary deposition processes which have recently been developed in our research department. We felt that this approach would give up the best chance of obtaining successfully results.

RESULTS

We coated three different combinations of materials which we felt had the best chance of surviving the high temperatures involved in the bake process. Unfortunately, none of the three samples survived the bake. The results of our bake tests at 1300°C are listed below, along with explanations of possible mechanisms which led to the failures.

Sample 1310-0093

The coating lost all color. No interference effects are observable in the remaining coating. The coating is still on the surface of the substrate. The mechanism operative here might be interdiffusion of the layers resulting in a homogeneous deposit.

Sample 1310-0094

The coating turned powdery and can be wiped off the substrate. Recrystallization of the coating materials could have led to an increase in film stresses and a loss of adhesive and cohesive strengths.

Sample 1310-0095

Some interference effects are still visible in this sample, though the optical performance is significantly degraded from the before-bake situation (compare scans of before and after bake). Once again, there may be some interdiffusion between layers. One encouraging aspect of this sample is that it remains firmly adhered to the substrate and it does not show any signs of crazing. The scatter level increased slightly, indicating some amount of recrystallization. This sample is, therefore, the best bet for a starting point for further work in high temperature coating for your purposes.

CONCLUSION

We were not able to find a coating combination which satisfies your requirement of surviving a bake at 1300°C. The coatings seemed to have failed from intrinsic material properties. This implies that varying the deposition parameters (CVD, evaporation, sputtering, etc.) will not have much of an effect on the results of a bake at these high temperatures. However, an earlier test run was baked at 1100°C, and showed considerably better performance. We therefore suggest that if the 1300°C requirement can be reduced to 1000°C or 1100°C, then we may be able to develop a design that can survive at the lower temperature.